Volume 2023, 17 pages | Article ID: IJETS-2310242112865

International Journal of Engineering & Technology Sciences

Journal homepage: http://htpub.org/IJETS/

ISSN 2289-4152

Investigating the Impact of Corrosion on Reinforced Concrete Frames with Corroded Steel Reinforcements

Amir Atashi, Hadi Einabadi[1]

Department of Civil Engineering, Technical and Vocational University (TVU), Tehran, Iran

Article

Article history:
Received: 11/06/2023
Received in revised form: 17/10/2023
Accepted: 24/06/2023

Keywords:
Corrosion,
Reinforced Concrete Frames,
Explosion,
Abaqus,
Steel Reinforcement

Abstract

This article focuses on the behavior of reinforced concrete frames with corroded steel reinforcements at different corrosion rates. To achieve this, the study delves into factors influencing corrosion, including the reduction of mechanical properties of steel reinforcements, the decrease in mechanical properties of concrete cover, and the decrease in the bond strength between steel reinforcements and concrete, to investigate the explosive behavior of these structures. Seven models with identical concrete frame geometries were analyzed in this study, with variations only in the rates of steel reinforcement corrosion and the affecting factors. Concrete frames with steel reinforcements corroded at rates of 5%, 10%, and 15%, considering the simultaneous and individual effects of reducing the mechanical properties of steel reinforcements, decreasing the mechanical properties of the concrete cover, and reducing the bond strength between steel reinforcements and concrete, were examined. The results indicate that the reduction in bond strength between steel reinforcements and concrete significantly reduces the resistance of concrete frames. Moreover, as the level of corrosion in the reinforcements increases, the extent of damage inflicted on the structure will significantly rise.

1. Introduction

Concrete is one of the most widely used and cost-effective materials in the construction of buildings, bridges, and many different structures worldwide. The reason for the extensive use of concrete is its strength and affordability. As we know, concrete is a material that is weak in tension and bending but highly resistant to compression. To compensate for this weakness, concrete structures are primarily reinforced with steel rebars to provide sufficient resistance against tensile and flexural loads and prevent cracking and failure. With advances in science, various methods for strengthening structures and their columns against seismic and explosive loads have been proposed. Research by (Zadeh et al., 2023) suggests that recycled concrete can be used for reinforcing concrete structures, promoting

[1]Corresponding author at: Technical and Vocational University (TVU), Tehran, Iran.
Email address: hadi.einabadi64@gmail.com

sustainability, and addressing environmental concerns. This method reduces the demand for virgin concrete and can be used in retrofitting projects, contributing to cost-effectiveness and eco-friendliness in the construction industry. While the use of steel rebars strengthens concrete structures, it also leads to corrosion issues over time, which can weaken, damage, and ultimately lead to the failure of the structure. Corrosion of steel rebars in concrete structures results from three main reasons, which are a reduction in the cross-sectional area and properties of the steel rebars, a decrease in the bond strength between the steel rebar and the concrete due to corrosion, and the development of cracks in the external concrete cover, known as a concrete cover, leading to a reduction in the properties of the concrete in this area (Du et al., 2005; Gonzalez et al., 1995). Ensuring that structures stay stable under varying loads is the primary goal of structural design in the modern era. As a result of that, these days, the improvement of the stability of structures under various loads is one of the most significant issues. In order to reinforce the structures, researchers are working on enhancing the material properties (Ferdosi & Porbashiri, 2022). In response to this issue, some researchers are actively looking into different approaches and tactics to increase the durability of structures under varied loads. For example, transverse reinforcements were added to the outer tube of elliptical CDFST (Concrete-Filled Double-Skin Tube) columns in the study to better understand their buckling behavior. Scientists modeled elliptical columns subjected to compressive stress using Abaqus software for their investigation. The investigation's conclusions confirm the stability of these columns under load by demonstrating a significant improvement in load-bearing capacity, particularly for columns with transverse reinforcements (Mohammed Ali et al., 2024). Akbari et al. (2013) used ABAQUS finite element software to predict the seismic performance of composite reinforced concrete and steel (RCS) joints under cyclic and uniform stresses. A revised model was introduced, which had more capacity and demonstrated more consistent behavior, making the system more appealing (Nazeryan & Feizbahr; Toosi & Ahmadi, 2023). The behavior of a shape memory alloy brace frame under explosive loads that is buckling constrained is examined by (Sadeghipour & Khorramabadi). The simulation and validation processes were carried out using the program ABAQUS. Sadeghipour (2023) investigates, despite the paucity of information, the explosive behavior of reinforced concrete frames retrofitted with wasp nest dampers, a relatively new type of damper, in order to determine its efficacy in minimizing structural damage under explosive situations.

Apart from other potential issues encountered over the lifetime of steel structures, such as fatigue and brittle fracture, which have been extensively studied by (Moradi et al., 2021), corrosion of steel reinforcements in concrete structures, especially in bridges, costs approximately $3.8 billion annually. This cost includes the replacement and maintenance of deteriorated bridges. The indirect costs, such as traffic disruption, can be estimated to be about ten times this figure (Pour-Ali et al., 2015). In addition to the financial costs, the structural damage resulting from the corrosion of concrete structures also has significant implications. Repair, maintenance, and rehabilitation of corroded reinforced concrete structures incur substantial expenses (Li & Melchers, 2005).

Considerable research has been conducted on the tensile properties of corroded steel reinforcements. Two types of corrosion are typically distinguished: natural corrosion (as seen in older structures) and accelerated corrosion, induced artificially through electrochemical methods for comprehensive tensile testing of rebars. Most of these tests show a significant reduction in yield and ultimate tensile stresses as well as ultimate strain (Kashani et al., 2013; Zhang et al., 2012).

When the external layer of steel rebar corrodes, the moisture in the environment can easily deteriorate it. Corrosion has a substantial impact on reducing the lifespan and serviceability of a structure compared to what was initially expected during the project. When the corrosion process

begins, the reconstruction of the structure becomes very costly. Hence, prevention during the design and implementation phases would be far less expensive. The reduction in load-bearing capacity of a member in a reinforced concrete structure due to corrosion is typically due to the following factors:

1. Reduction in the effective cross-sectional area of concrete due to cracking and separation of the concrete cover.
2. Decrease in the cross-sectional area and flexibility of the rebars.
3. Reduced bond strength between the steel and concrete, leading to debonding of separated rebars from the concrete.

Habibi (2017) in the conclusion of his master's thesis presented at the University of Toronto in Canada, addressed the presentation of a finite element model of damage in reinforced concrete structures. He used the VecTor2 software to code the formulation provided in this thesis and investigated the corrosion process in concrete beams with simple supports. He compared and validated the research results with laboratory experiments. He stated that corrosion can generally be divided into two categories: uniform and pitting corrosion, and factors that reduce the resistance of reinforced concrete structures due to corrosion fall into three categories: reducing the resistance and cross-sectional area of steel bars, reducing the bond strength between concrete and steel bars, and reducing the properties of concrete cover. For each section, he presented specific formulations based on the corrosion intensity and implemented these formulations in the software, conducting simulations.

Zhao et al. (2018) conducted a numerical analysis of the reduction in capacity of reinforced concrete beams under the influence of corroded steel bars. They used Abaqus software to examine and simulate corrosion in steel bars. They presented a relationship for the CDP model used to simulate concrete in Abaqus for predicting the stress-strain curve and damage for concrete. They then modified this relationship for corroded concrete based on the corrosion rate. After presenting the concrete simulation relationships, they provided a formulation based on connector elements to simulate the reduction in bond strength between steel bars and concrete using a non-linear spring. Finally, they presented relationships for reducing the cross-sectional area and mechanical properties of corroded steel bars for implementation in Abaqus. They studied three levels of corrosion, including 5%, 10%, and 15%, and extracted the relevant values and parameters for these three types of corrosion for use in Abaqus. They compared the simulation model in their research with laboratory results and rigorously validated the research process.

Zabihi-Samani et al. (2018) simulates the behavior of reinforced concrete beams with corroded steel bars and ultimately strengthened these beams using CFRP. They considered 20% and 40% corrosion in the steel bars and, following the method used by Zhao et al. (2018), simulated the reduction in bond strength between steel bars and concrete. After examining concrete beams with corroded steel bars and validating their results, they presented a solution and used CFRP to strengthen the corroded concrete beams.

Du et al. (2006) used finite element analysis to investigate the effects of radial expansion of strengthening corroded steel bars on crack formation in concrete. They studied the impact of the radial expansion of the steel bars resulting from corrosion product formation on crack formation in the concrete cover. Their research involved a transition from a three-dimensional model to a two-dimensional shell model, and they performed their analyses on this sample. Their results showed that the radial expansion of corroded steel bars led to crack formation in the concrete cover in four different stages, which are internal cracking, external cracking, crack propagation, and final cracking.

Berra et al. (2003) studied the finite element method to examine the force transfer between corroded steel bars and concrete at different corrosion levels. They investigated the influence of corrosion on the bond strength between corroded steel bars and concrete using finite element analysis with a symmetrical axial model at different corrosion levels and compared their research results with experimental results.

2. Research Foundation

In this section, the formulation and simulation of corrosion in steel bars using Abaqus software are discussed. Following this, the process of simulating and validating the model is outlined, and, finally, the main models of this research will be presented.

2.1. Changes in Mechanical Properties of Corroded Steel Bars

In general, there are two types of corrosion: uniform corrosion and pitting corrosion. In uniform corrosion, the cross-sectional size and shape of the steel bar do not change along its length, which is the ideal condition. However, in pitting corrosion, the issues that arise are much more complex, and the cross-sectional area and geometry do not change uniformly along the length of the bar. Therefore, implementing this type of corrosion is very challenging and is usually modeled using a set of equations based on the assumption of uniform corrosion. Based on this, with the knowledge of the volume loss due to corrosion, which can be obtained from equations provided based on the intensity and type of corrosion, the reduction in mechanical properties can be determined as follows. (Wang & Liu, 2008) presented the following relationship for yield stress and elastic modulus of corroded steel bars:

$$f_{yc} = (1 - 0.00198\delta) f_y$$
$$E_{sc} = (1 - 0.00113\delta) E_s \quad (1)$$

In this equation, fy represents the yield stress of intact steel bars, Es is the elastic modulus of intact steel bars, δ is the rate of mass loss in corroded steel bars, fyc stands for the yield stress of corroded steel bars, and Esc is the elastic modulus of corroded steel bars. Wang and Liu (2008) proposed the following relationship for the ultimate stress and ultimate strain of corroded steel bars:

$$f_{uc} = (1.0 - 0.019\delta) f_u$$
$$\varepsilon_{uc} = (1 - 0.021\delta) \varepsilon_u \quad (2)$$

Where fu represents the ultimate stress of intact steel bars, fuc is the ultimate stress of corroded steel bars, εu is the ultimate strain of intact steel bars, and εuc is the ultimate strain of corroded steel bars. Considering the three corrosion rates presented in the paper by (Wu & Yuan, 2008), the values for intact and corroded steel bars based on 5%, 10%, and 15% corrosion levels are provided in Tables 1 and 2, respectively. In this study, two types of steel for the bars and ties have been used, and the properties of these two types of steel are presented in Table 1 throughout the paper.

Table 1. Properties of Intact Steel Bars (Wu & Yuan, 2008).

Type of rebar	Es (MPa)	fy (MPa)	fu (MPa)	εu
HPB235	210000	258.25	393.39	0.15
HRB235	200000	373.71	578.28	0.15

Table 2. Properties of Corroded Steel Bars at Three Levels: 5%, 10%, and 15% (Wu & Yuan, 2008).

Corrosion rate of rebar section	Es (MPa)	fy (MPa)	fu (MPa)	εu(MPa)
Diameter of rebar D=12 mm				
0%	210000	258.25	393.39	0.15
5%	197769.7	231.90	354.87	0.13
10%	185829.1	206.17	317.26	0.12
15%	172889.8	178.28	276.50	0.10
Diameter of rebar D=20 mm				
0%	200000	373.71	578.28	0.15
5%	188500.8	336.06	522.38	0.13
10%	176835.3	297.87	465.66	0.12
15%	164508.9	257.51	405.73	0.10

2.2. Reduction in Bond Force between Steel Bars and Concrete

To simulate intact steel bars and ties in concrete, the Embedded Region constraint is typically used. However, instead of using this constraint, it is often possible to utilize the stress-displacement relationship between steel bars and concrete presented in Figure 1. This approach is employed for simulating the behavior of steel bars and ties embedded in concrete, especially in the absence of the Embedded Region constraint.

For simulating the forces and interactions between steel bars and concrete, a connector element with axial force in the form of a spring can be used. This approach adequately simulates the frictional effects between steel bars and concrete. The usage of the spring element for simulating the force between steel bars and concrete is presented in Figure 2.

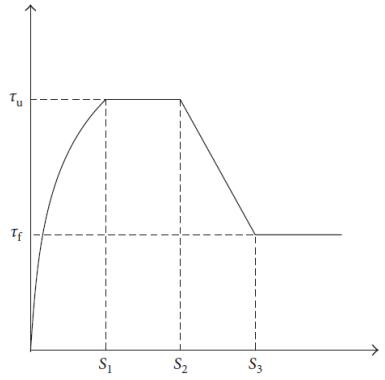

Figure 1. Stress-Displacement Relationship between Steel Bars and Concrete (Wu & Yuan, 2008).

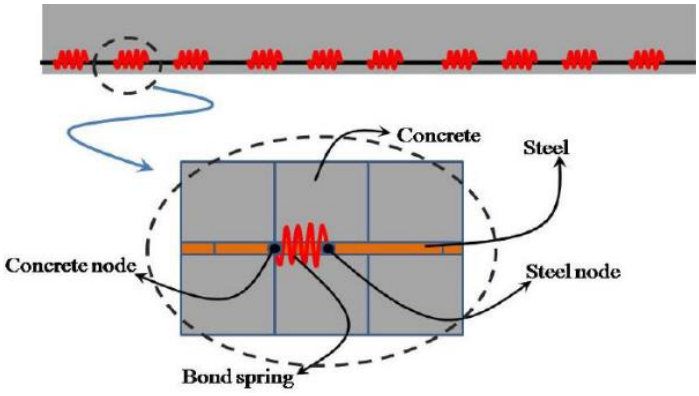

Figure 2. Simulation of the Force between Steel Bars and Concrete Using a Spring Element (Zabihi-Samani et al., 2018).

As shown in Figure 1, to create the force-displacement curve in this figure, you require five parameters. These parameters for intact steel bars are provided in Table 3.

Table 3. Parameters for Simulation of the Joint Behavior between Intact Steel Bars and Concrete as a Nonlinear Spring Element in Abaqus (Wu & Yuan, 2008).

S1	S2	S3	α	τu	τf
1.0 mm	3.0 mm	Rib spacing	0.4	$2.5\sqrt{f_c}$	0.4τu

In this table, fc represents the maximum tensile strength of concrete. For corroded steel bars, the values of τf and τu decrease, and the magnitude of this reduction can be calculated using the following formulas (Apostolopoulos & Papadakis, 2008).

$$\theta = \frac{\tau_u^{cor}}{\tau_u} = 0.9959e^{0.0041\delta} + 0.0069e^{0.7858\delta}, \delta \le 4\% \qquad (3)$$

$$\theta = \frac{\tau_u^{cor}}{\tau_u} = 9.662e^{-.5552\delta} + 0.1887e^{0.0069\delta}, \delta > 4\%$$

Table 4. Values of Changes in Stresses for the Joint Behavior between Corroded Steel Bars and Concrete for Joint Simulation in Abaqus (Wu & Yuan, 2008).

Corrosion rate of rebar section	0%	5%	10%	15%
τu (MPa)	14.7	11.0	3.7	2.9
τf (MPa)	5.9	2.2	2.2	2.2

2.3. Reduction in Cover Region Properties

For a better understanding of the cover region in concrete, please refer to Figure 3. Based on the theories presented in the articles, the generation of corrosion products and the resulting pressure exerted by these products, as well as the fact that this pressure cannot penetrate the internal section, influence the outer cover region. This leads to the development of cracks in the cover region and a significant reduction in its properties.

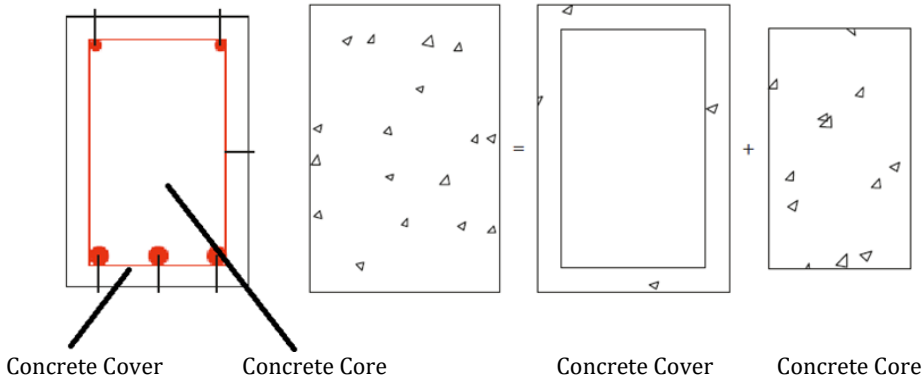

Figure 3. The difference between the concrete core and cover (Wu & Yuan, 2008).

To reduce the properties in this region, the reference article (Wu & Yuan, 2008) suggests the following relationships. Before discussing these relationships, considering that the Abaqus software employs the Concrete Damage Plasticity (CDP) model for simulating concrete behavior, and for an accurate simulation of concrete behavior, the software requires the stress-strain diagrams for both tension and compression, as well as the damage and pressure parameters. Initially, this article presents the following relationship for determining the stress-strain diagram in the compression region:

$$\sigma_c = \frac{((E_c / E_g)(\varepsilon / \varepsilon_c)) + (D-1)(\varepsilon / \varepsilon_c)^2}{1 + ((E_c / E_g) - 2)(\varepsilon / \varepsilon_c) + D(\varepsilon / \varepsilon_c)^2} f_c \qquad (4)$$

$$E_g = \frac{f_c}{\varepsilon_c}$$

In this relationship, "fc" represents the maximum compressive stress at the peak of the stress-strain curve, and "εc" is the peak strain, typically assumed to be 0.002. Additionally, "EC" denotes the initial elastic modulus of concrete, which can be calculated using the well-known Mandel relationship: EC = 5000(fc)^0.5. Furthermore, "D" in this relationship is the pressure softening adjustment parameter, which is a value between zero and one. The stress-strain diagram for various "D" values is presented in Figure 4. In the tensile region, the stress-strain diagram for concrete can be calculated as follows.

$$\sigma_t = \begin{cases} yf_t & y \le 1 \\ \left(\dfrac{\beta y f_t}{\beta - 1 + y^{\beta}} \right) & y \ge 1 \end{cases} \qquad (5)$$

$$y = \frac{\varepsilon}{\varepsilon_t}$$

In this equation, εt = ft / Ec, where typically ft = 0.1 * fc, and β is the tensile region adjustment parameter, which is usually greater than one. The stress-strain diagram for tensile concrete based on various values of β is presented in Figure 5.

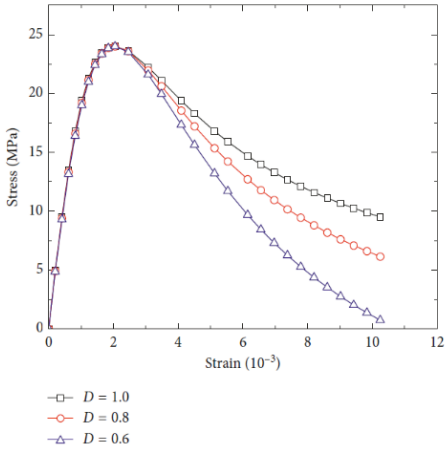

Figure 4. Stress-Strain Curve for Compression Based on Different "D" Values (Wu & Yuan, 2008).

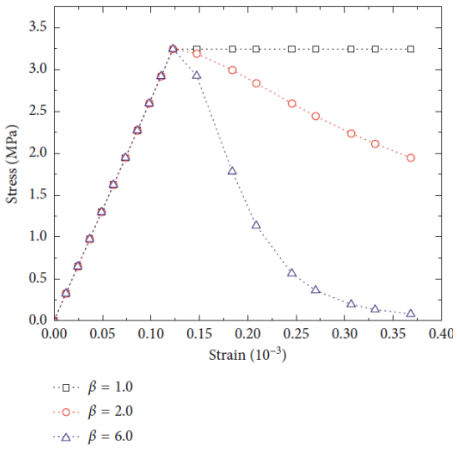

Figure 5. Tensile Stress-Strain Curve Based on Various Values of β (Wu & Yuan, 2008)

The damage parameter in the Abaqus software is a value that ranges between zero and one. A value of zero implies no damage, while a value of one indicates complete failure. The following formulas are used for calculating tensile and compressive damage in the Abaqus software.

$$d = 1 - \frac{\sigma_{true} E_c^{-1}}{\varepsilon^{pl}(1/b_{c/t} - 1) + \sigma_{true} E_c^{-1}}$$

$$\varepsilon_{true} = \ln(1+\varepsilon)$$

$$\sigma_{true} = \sigma(1+\varepsilon) \qquad (6)$$

$$\varepsilon^{in} = \varepsilon_{true} - \frac{\sigma_{true}}{E_c}$$

$$\varepsilon^{pl} = b_{c/t}\varepsilon^{in}$$

In this equation, "d" represents the damage parameter in the tensile or compressive region, and "b" is the scaling parameter between the non-elastic and plastic strain. For the tensile region, "b" is typically taken as 0.3, and for the compressive region, it's typically taken as 0.7. Now, after presenting the required equations for calculating parameters and stress-strain curves, as well as tensile and compressive damage for simulation in the Abaqus software, it is necessary to reduce the values associated with stresses and strains resulting from corrosion. To calculate these values, the following equations are used.

$$f_{c-cor} = \frac{f_c}{1+\gamma(\varepsilon_{t-cor}/\varepsilon_c)}$$

$$\varepsilon_{t-cor} = \frac{b_{cor}-b}{b}$$

$$b_{cor} = b + nw_{cor} \tag{7}$$

$$w_{cor} = \sum_i u_{icor} = 2\pi(v_{cor}-1)X$$

$$\rho_s = \frac{2X}{r}(\frac{X}{r})^2$$

In these equations:

- "fc" and "fc-cor" represent the maximum compressive stress for undamaged and corroded rebars, respectively, with the correction factor equal to 1.0.
- "εc" and "εt-cor" are the strains at the point of maximum stress for sound and corroded rebars, respectively.
- "b" and "bcor" are the initial width and width of the corroded member, respectively.
- "N" is the number of tendons and longitudinal bars subjected to corrosion.
- "wcor" is the total width of corrosion cracks.
- "vcor" is the penetration factor of corrosion products, typically equal to 2.
- "uicor" is the width of the corrosion crack in member i.
- "X" is the depth of rebar corrosion.
- "ρs" is the corrosion rate of the cross-sectional area.
- "R" is the radius before surface corrosion of the rebar.

You can calculate "ρs" using the following formula.

$$\rho_s = \begin{cases} 0.013+0.987\delta & \delta \le 10\% \\ 0.061+0.939\delta & 10\% < \delta \le 20\% \\ 0.129+0.871\delta & 20\% < \delta \le 30\% \\ 0.199+0.810\delta & 30\% < \delta \le 40\% \end{cases} \tag{8}$$

Considering the equations and the three corrosion levels of 5%, 10%, and 15%, the values used for concrete cover affected by corroded rebars for the mentioned corrosion levels are presented in Table 5.

Table 5. Maximum Compressive Strength of Concrete Cover under Different Corrosion Rates (Wu & Yuan, 2008).

Corrosion rate of rebar section	0%	5%	10%	15%
Concrete compressive (MPa)	34.55	17.37	11.08	8.61

2.4. Validation of Finite Element Results in Abaqus Software

The geometry used in simulating a concrete beam is as follows: it has a length of 2400 millimeters and features a 25-millimeter concrete cover. The cross-sectional area is 200 by 300 millimeters, as shown in Figure 5. For reinforcement, 8-millimeter diameter stirrups spaced at 100-millimeter intervals are used, along with two rebars in the upper tensile zone with diameters of 12 millimeters, and three rebars in the lower compressive zone, two of which have a diameter of 20 millimeters and one with a diameter of 12 millimeters. The details of the cross-sectional area, the utilized rebars, loading conditions, and boundary conditions on the beam are fully provided in Figures 6 and 7.

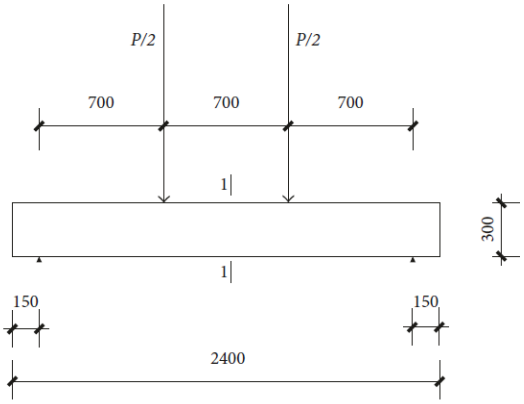

Figure 6. Schematic of the Beam with Boundary Conditions and Loading (Wu & Yuan, 2008).

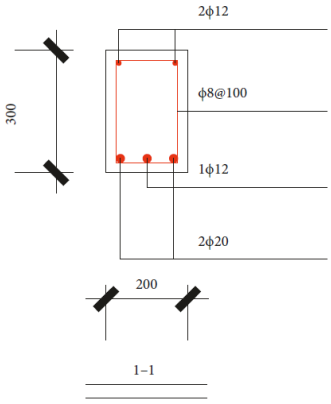

Figure 7. Cross-Sectional Details and Utilized Rebars for Validation Model (Wu & Yuan, 2008).

The concrete in the model is represented using the CDP (Concrete Damage Plasticity) model, and the reinforcement and stirrups are modeled using truss elements. The stirrups have a diameter of 20 millimeters and are made of HRB235 steel, while the rebars have a diameter of 12 millimeters and are made of HPB235 steel. The material properties for both sound and corroded conditions are provided in Tables 1 and 2.

The validation analysis was conducted using the Abaqus software for two scenarios. Model number 1 represents a configuration where both the reinforcement and stirrups are in sound condition. Model number 2, on the other hand, represents a scenario where all three parameters are considered: the reduction in properties of corroded rebars, the reduction in the bond force between rebars and concrete through the application of connectors, and the reduction in the concrete cover strength from 34 megapascals to 8 megapascals simultaneously, for a corrosion rate of 15 percent. In continuation of this research, seven additional models were analyzed. In all of these models, a reinforced concrete frame with a span and a story was subjected to explosive loads at a distance of 3 meters (equivalent to one span), and the corrosion parameters of the embedded rebars were altered in each model.

In Model 1, a sound reinforced concrete frame was analyzed. In Model 2, only the effect of the common bond force between the concrete and steel rebars due to 10% corrosion was considered. In Model 3, the impact of the mechanical property reduction of steel rebars under 10% corrosion was taken into account. In Model 4, a specific reduction in the concrete cover strength due to 10% corrosion was considered. The reason for analyzing Models 2 to 4 is to examine the individual influence of each of these corrosion factors on the behavior of the concrete frame under explosion loads. In Model 5, the simultaneous effect of all corrosion factors due to 5% corrosion was considered. In Model 6, the simultaneous effect of all corrosion factors due to 10% corrosion was taken into account. In Model 7, the simultaneous influence of the three corrosion factors with a 15% corrosion rate was considered. The specifications of the analyzed models in this research are provided in Table 6.

Table 6. Specifications of the 7 Analyzed Models in this Research.

Model No.1	Reinforced concrete frame
Model No.2	Reinforced Concrete Frame considering a 10% reduction in the common bond force between concrete and steel rebars due to corrosion.
Model No.3	Reinforced Concrete Frame considering a 10% reduction in the mechanical properties of steel rebars due to corrosion.
Model No.4	Reinforced Concrete Frame considering a 10% reduction in concrete cover strength due to corrosion.
Model No.5	Reinforced Concrete Frame considering all corrosion factors with a 5% corrosion rate.
Model No.6	Reinforced Concrete Frame considering all corrosion factors with a 10% corrosion rate.
Model No.7	Reinforced Concrete Frame considering all corrosion factors with a 15% corrosion rate.

In all of the models, the geometry of the reinforced concrete frame, as well as the specifications of the reinforcement and stirrups, remain consistent. The design of the reinforced concrete frame in this research is based on the ACI (American Concrete Institute) code. The concrete frame in this study has a span of 3 meters and a height of 3 meters. The beams and columns of the concrete frame have a cross-section of 30 x 30 centimeters. The dimensions of the stirrups are 25 x 25 centimeters, and the rebars have a length of 3 meters. The geometry of the concrete frame and reinforcement arrangement is presented in Figures 8 and 9.

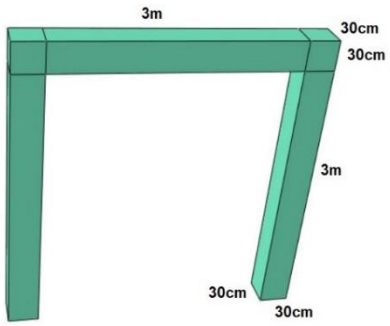

Figure 8. Geometry of the Reinforced Concrete Frame Analyzed in this Research.

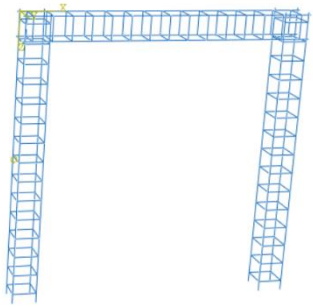

Figure 9. Assembly Model of the Reinforcement and Stirrups in Different Models.

Similar to the validation case for the rebars and stirrups, truss elements were used for the connections, and the rebars had a diameter of 12 millimeters, while the stirrups had a diameter of 20 millimeters. The support conditions for the model in the lower part are fully constrained, as shown in Figure 10, and an explosive load, as depicted in Figure 11, was applied to the model from a distance of 3 meters on the left side, with a magnitude of 30 kilograms TNT equivalent.

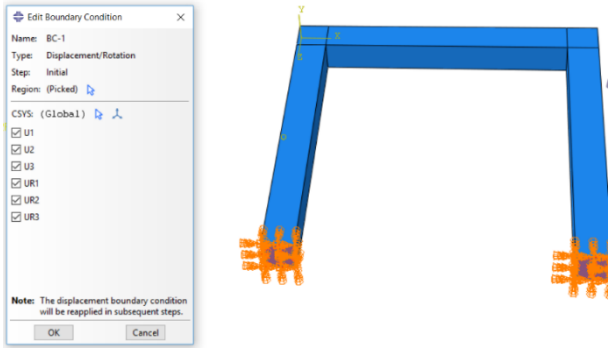

Figure 10. Restraining the Bottom Part of the Reinforced Concrete Frame.

A mesh size of 50 millimeters was used for discretizing the reinforced concrete frame, rebars, and stirrups. The element employed for the reinforced concrete frame is C3D8R, which is an 8-node three-dimensional element. The elements used for the rebars, and stirrups are truss elements. The meshed model of the reinforced concrete frame is illustrated in Figure 12.

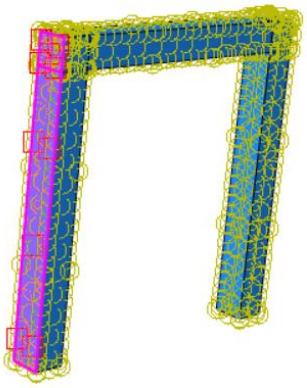

Figure 11. Explosion Initiation Point and the Surface of the First Impact of the Blast Wave on the Reinforced Concrete Frame.

Figure 12. Meshing of the Reinforced Concrete Frame.

3. Discussion and Results

3.1. Validation Results

The results for the 2 analyzed cases in the Abaqus software for the validation section and their comparison with the reference paper (Wu & Yuan, 2008) are presented in Figures 13 and 14. As observed, the load-carrying capacity of the beam in the intact condition is 260 kilonewtons, and the results obtained show good agreement with the results of the reference article (Wu & Yuan, 2008), with a difference of less than 5 percent.

As observed, the load-carrying capacity of the beam in the case where all three parameters affecting corrosion (i.e., reduction in the mechanical properties of reinforcing bars due to corrosion by 15%, reduction in the bond strength between corroded rebars and concrete, and reduction in concrete cover strength due to 15% corrosion) is applied, has decreased from 260 kilonewtons for the healthy sample to 160 kilonewtons. The results obtained show good agreement with the results of the reference article (Wu & Yuan, 2008), with a difference of less than 5 percent.

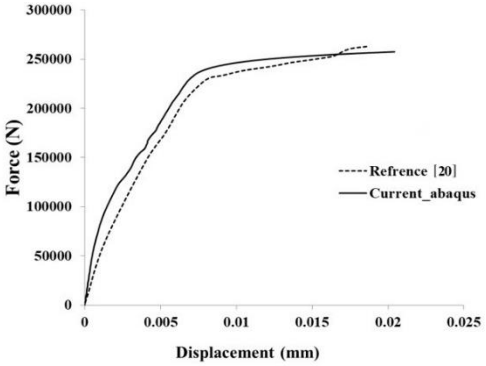

Figure 13. Comparison of results between the reference (Wu & Yuan, 2008) and Abaqus analysis in this study for the intact specimen.

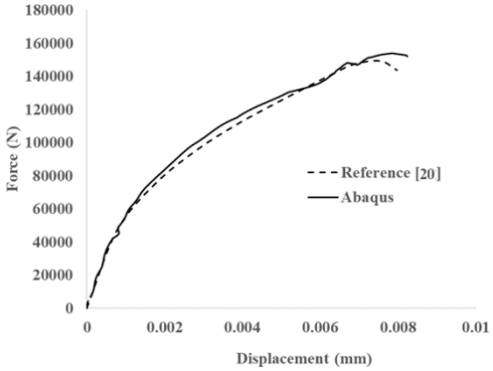

Figure 14. Comparison of results between the reference (Wu & Yuan, 2008) and Abaqus analysis in this study for Sample No. 24 (simultaneous effects of three parameters: reduction in mechanical properties of corroded rebars, reduction in the bond strength between corroded rebar and concrete, and reduction in concrete cover strength for a corrosion rate of 15 percent).

3.2. Presentation of Results for Other Analyzed Models in This Research

The results related to the 7 analyzed models in this article are presented in this section. The results obtained for comparison include horizontal and vertical displacements, as well as the damage extent in the analyzed frames. The results for model number 1 are presented in Figure 15.

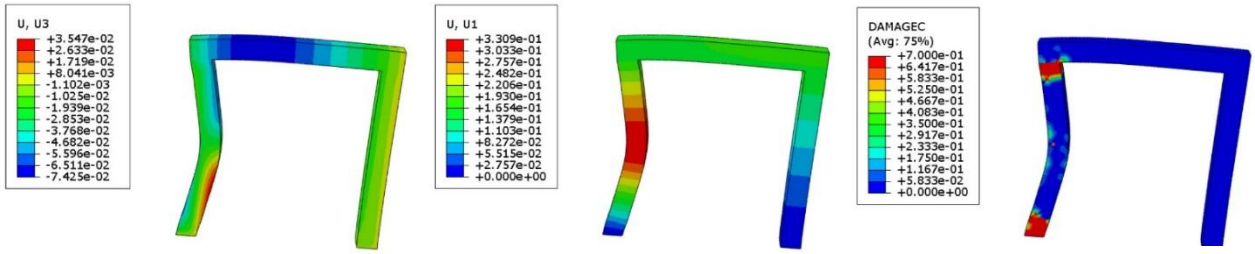

Vertical Displacement | Horizontal Displacement | The extent of damage

Figure 15. Horizontal and vertical displacements, as well as the extent of damage in Model 1 (Undamaged model)

As seen in Figure 15, the maximum horizontal displacement due to the blast load in Model 1, which is healthy and without corrosion, is 33 centimeters, and the maximum vertical displacement is 74 millimeters. Also, the damage contour has a higher value in the areas of the left support and at the section level change, with lower values in the remaining areas. Moreover, the damaged areas in the healthy sample cover only a few sections of the structure. Next, in Figure 18, the results for Model 2, which considers only the parameter of reducing the bond strength between steel rebars and concrete due to 10% corrosion in the sample, are presented. As mentioned in Figure 16, the maximum horizontal displacement in this model is 1.41 cm, and the maximum vertical displacement is 4.12 cm, which represents an increase of 24% in horizontal displacement and 67% in vertical displacement compared to the reference model (Model 1, the intact model). The extent of damage and compressive failure has also increased compared to the reference model (Model 1, the intact model). Middle areas of the column have been affected by damage and failure. This is primarily due to the increased displacements in this region in this model compared to Model 1, which has resulted in an increased level of structural damage.

In the following Figure 19, the results for Model 3, considering only the reduction in the mechanical properties of steel rebars under 10% corrosion in the specimens, are presented.

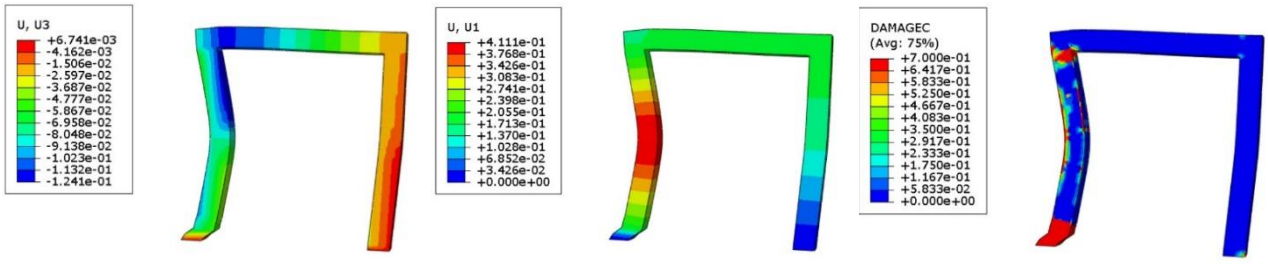

Vertical Displacement Horizontal Displacement The extent of damage

Figure 16. Horizontal and vertical displacements and damage extent in Model 2 (10% corrosion, considering only the parameter of reducing the bond strength between steel rebars and concrete).

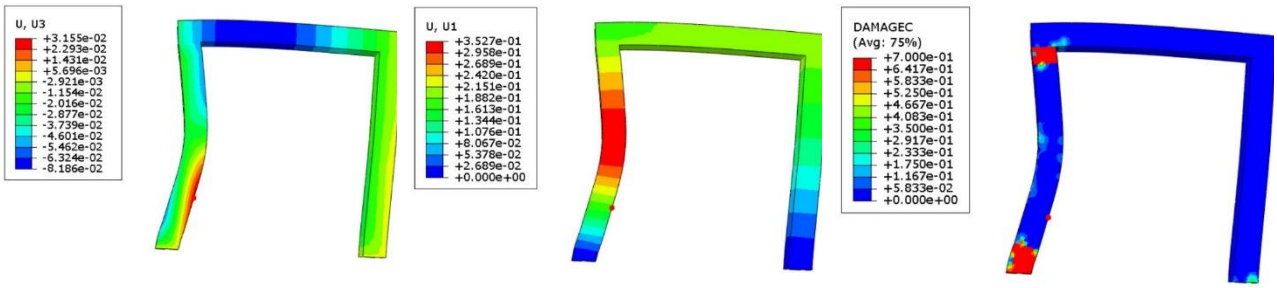

Vertical Displacement Horizontal Displacement The extent of damage

Figure 17. Horizontal displacement, vertical displacement, and damage extent in Model 3 (10% corrosion with only the consideration of the reduction in the mechanical properties of steel rebars).

Figure 17 shows that the maximum horizontal displacement in Model 3 is 2.35 cm, and the maximum vertical displacement is 8.1 cm. The results indicate a 6.6% increase in horizontal displacement and a 4.9% increase in vertical displacement compared to the reference model (Model 1, undamaged model). These results demonstrate that the influence of this factor, the reduction in the mechanical properties of steel rebars due to corrosion, is significantly greater than the effect of the factor considered in Model 2 (reduction in the bond strength between rebars and concrete). Continuing to Figure 20, the results for Model 4 are presented.

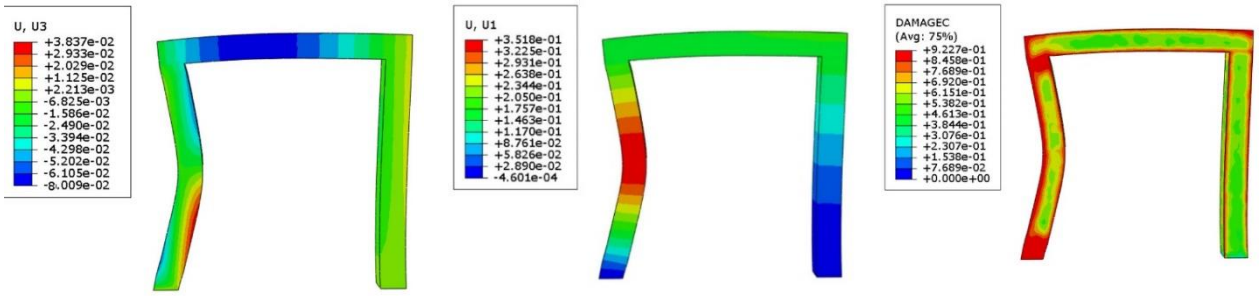

Vertical Displacement Horizontal Displacement The extent of damage

Figure 18. displays the results for Model 4, which considers only the reduction in the mechanical properties of concrete cover due to a 10% reduction in corrosion.

As shown in Figure 18, the horizontal and vertical displacements in Model 4 are 35/18 centimeters and 80 millimeters, respectively. This represents a 6.6% increase in horizontal displacement and a 9-millimeter increase in vertical displacement compared to the reference model. The effect of this factor

is similar to the reduction in mechanical properties of steel rebars due to corrosion, and these two factors have a less significant impact compared to the reduction in the common force between steel and concrete. Furthermore, the increased damage in the structure is mainly due to the reduction in the mechanical properties of the concrete cover, which leads to more damage in the outer concrete sections. Continuing with Figure 19, the results for Model 5, which considers the simultaneous effect of the three parameters: reduction in the mechanical properties of steel rebars, reduction in the common force between steel rebars and concrete, and reduction in the mechanical properties of the concrete cover with a corrosion rate of 5%, are presented.

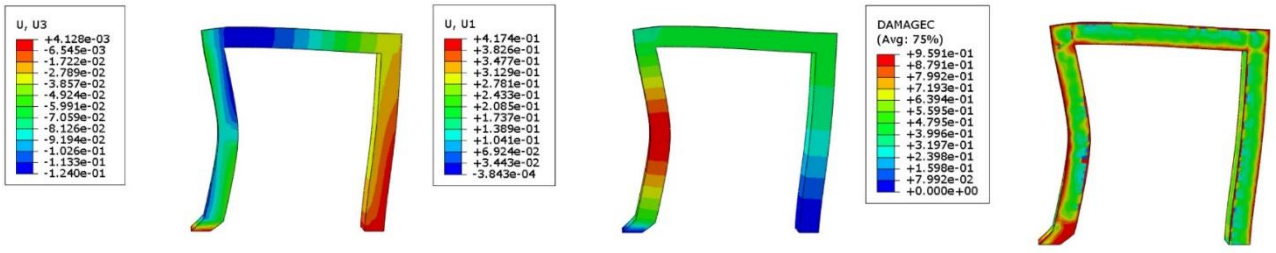

Vertical Displacement Horizontal Displacement The extent of damage

Figure 19. Horizontal and vertical displacements, as well as the extent of damage in Model 5 (5% corrosion rate, considering the simultaneous effect of three influential corrosion factors).

As shown in Figure 19, the maximum horizontal displacement in this model is 41.74 cm, and the vertical displacement is 12.4 cm. As can be seen from the obtained values, the horizontal displacement has increased by 26.5% compared to the reference model, and the vertical displacement in this model has increased by 67.5% compared to the reference model. Moreover, the damage zones in this model have expanded compared to the reference model, with significant damage in the concrete cover area, where concrete properties have been reduced. Next, the results for Model 6 are presented.

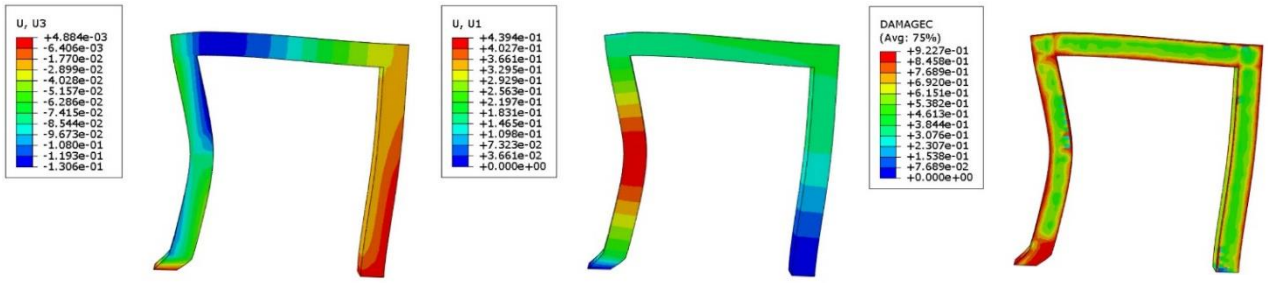

Vertical Displacement Horizontal Displacement The extent of damage

Figure 20. Horizontal Displacement, Vertical Displacement, and Damage extent in Model Number 6 (10% Corrosion, Considering Three Simultaneous Corrosion-Related Factors)

As seen in Figure 20, the horizontal displacement in this model is 9.43 centimeters, and the vertical displacement is 130 millimeters, which represents a 33% increase in horizontal displacement and a 6.75% increase in vertical displacement compared to the reference model. Additionally, the displacement values in this model, with 10% corrosion, are higher than the previous model with 5% corrosion, both in horizontal and vertical displacements. Furthermore, it's evident that the compressive damage in this model is higher compared to the reference model and the model with 5% corrosion, indicating more structural damage at higher corrosion rates. Continuing with Figure 21, the final results

related to a model that considers the simultaneous impact of three influential corrosion parameters at a 15% corrosion rate are presented.

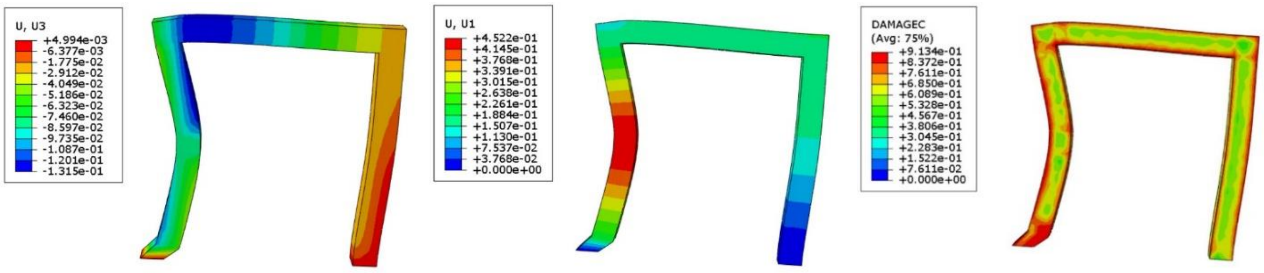

Vertical Displacement | Horizontal Displacement | The extent of damage

Figure 21. Horizontal Displacement, Vertical Displacement, and Damage extent in Model No. 7 (15% Corrosion, Considering Three Simultaneous Corrosion-Affecting Factors).

As shown in Figure 21, the maximum horizontal displacement in this model is 22.45 centimeters, and the vertical displacement is 145 millimeters. These values represent a 37% increase in horizontal displacement and a 77.77% increase in vertical displacement compared to the reference model. Additionally, both horizontal and vertical displacements in this model have increased compared to the reference model and models with 5% to 10% corrosion. Moreover, the damage level in this model has significantly increased compared to the reference model and models with 5% and 10% corrosion. This indicates that with an increase in the corrosion rate, the structural resistance is significantly reduced, and its strength against imposed loads will be weakened.

4. Conclusion

This article has investigated the explosive behavior of reinforced concrete frames with corroded rebars at different corrosion rates. Based on the conducted research, it has been established that the introduction of corrosion in steel rebars leads to a reduction in the structural performance of concrete structures under explosive loading. Throughout this study, seven models were analyzed, and the characteristics of these models have been thoroughly explained in the article. The following results can be extracted from the analyses performed in this paper:

1. Corrosion at any rate results in a decrease in the structural strength and deterioration of the concrete structure under explosive loading.
2. Among the three parameters affecting corrosion, the parameter of reducing the bond strength between steel rebars and concrete has the most significant impact on causing structural failure and reducing the structural strength, while the other two parameters have almost equal effects on the reduction in structural strength.
3. The horizontal displacement of the structure increases with a corrosion rate of 5% by 26.5%, a corrosion rate of 10% by 33%, and a corrosion rate of 15% by 45.2% compared to the undamaged specimen under an explosion with constant values.
4. Additionally, the vertical displacement increases by 67.5% at a corrosion rate of 5%, by 76.5% at a corrosion rate of 10%, and by 77.7% at a corrosion rate of 15% compared to the undamaged specimen under explosive loading.

These findings emphasize the detrimental effects of rebar corrosion on the structural behavior of reinforced concrete frames subjected to explosive loading.

References

Akbari, A., Nikookar, M., & Feizbahr, M. (2013). Reviewing Performance of Piled Raft and Pile Group Foundations under the Earthquake Loads. *Research in Civil and Environmental Engineering, 1*(5), 287-299.

Apostolopoulos, C. A., & Papadakis, V. (2008). Consequences of steel corrosion on the ductility properties of reinforcement bar. *Construction and Building Materials, 22*(12), 2316-2324.

Berra, M., Castellani, A., Coronelli, D., Zanni, S., & Zhang, G. (2003). Steel–concrete bond deterioration due to corrosion: finite-element analysis for different confinement levels. *Magazine of Concrete Research, 55*(3), 237-247.

Du, Y., Chan, A., & Clark, L. (2006). Finite element analysis of the effects of radial expansion of corroded reinforcement. *Computers & structures, 84*(13-14), 917-929.

Du, Y., Clark, L., & Chan, A. (2005). Effect of corrosion on ductility of reinforcing bars. *Magazine of Concrete Research, 57*(7), 407-419.

Ferdosi, S., & Porbashiri, M. (2022). Calculation of the Single-Walled Carbon Nanotubes' Elastic Modulus by Using the Asymptotic Homogenization Method. *International Journal of Science and Engineering Applications, 11*(12), 254-265.

Gonzalez, J., Andrade, C., Alonso, C., & Feliu, S. (1995). Comparison of rates of general corrosion and maximum pitting penetration on concrete embedded steel reinforcement. *Cement and concrete research, 25*(2), 257-264.

Habibi, S. (2017). *Finite element modelling of corrosion damaged reinforced concrete structures*: University of Toronto (Canada).

Kashani, M. M., Crewe, A. J., & Alexander, N. A. (2013). Nonlinear stress–strain behaviour of corrosion-damaged reinforcing bars including inelastic buckling. *Engineering Structures, 48*, 417-429.

Li, C. Q., & Melchers, R. E. (2005). Time-dependent risk assessment of structural deterioration caused by reinforcement corrosion. *ACI Structural Journal, 102*(5), 754.

Mohammed Ali, A., Besharat Ferdosi, S., Kareem Obeas, L., Khalid Ghalib, A., & Porbashiri, M. (2024). Numerical study of the effect of transverse reinforcement on compressive strength and load-bearing capacity of elliptical CFDST columns. *Journal of Rehabilitation in Civil Engineering, 12*(1).

Moradi, H., Rafi, R., & Muslim, A. (2021). Crack growth simulation in 13th row of compressor blades under foreign object damage and resonant vibration condition. *Journal of Vibroengineering, 23*(1), 44-62.

Nazeryan, M., & Feizbahr, M.(2022). Seismic Evaluation of the Cheng and Chen Modified Model Using Shear Keys in Steel Beam-to-Concrete Column Connections. *Computational Research Progress In Applied Science & Engineering, 8(2), 1-6*

Pour-Ali, S., Dehghanian, C., & Kosari, A. (2015). Corrosion protection of the reinforcing steels in chloride-laden concrete environment through epoxy/polyaniline–camphorsulfonate nanocomposite coating. *Corrosion Science, 90*, 239-247.

Sadeghipour, A. (2023). Investigation of concrete structures with wasp nest dampers against explosive loads.

Sadeghipour, A., & Khorramabadi, R. Analyzing the Explosive Behavior of a Buckling Restrained Brace Frame Made of Shape Memory Alloy by Using Finite Element Method.

Toosi, G., & Ahmadi, M. M. (2023). *Robust Process Capability Indices for Multivariate Linear Profiles.* Paper presented at the 2023 Systems and Information Engineering Design Symposium (SIEDS).

Wang, X.-h., & Liu, X.-l. (2008). Modeling the flexural carrying capacity of corroded RC beam. *Journal of Shanghai Jiaotong University (Science), 13*, 129-135.

Wu, Q., & Yuan, Y. (2008). Experimental study on the deterioration of mechanical properties of corroded steel bars. *China civil engineering journal, 41*(12), 42-47.

Zabihi-Samani, M., Shayanfar, M., Safiey, A., & Najari, A. (2018). Simulation of the behavior of corrosion damaged reinforced concrete beams with/without CFRP retrofit. *Civil Engineering Journal, 4*(5).

Zadeh, S. S., Joushideh, N., Bahrami, B., & Niyafard, S. (2023). A review on concrete recycling. *World Journal of Advanced Research and Reviews, 19*(02), 784-793.

Zhang, W., Song, X., Gu, X., & Li, S. (2012). Tensile and fatigue behavior of corroded rebars. *Construction and Building Materials, 34*, 409-417.

Zhao, G., Xu, J., Li, Y., & Zhang, M. (2018). Numerical analysis of the degradation characteristics of bearing capacity of a corroded reinforced concrete beam. *Advances in Civil Engineering, 2018*.